Responses to reviewer #3

Dear Editor and Reviewer #3:

We would like to thank the Editor and the reviewers for their time and valuable suggestions on our manuscript, "Optimizing Ammonia Emissions for $PM_{2.5}$ Mitigation: Environmental and Health Co-Benefits in Eastern China" (egusphere-2025-1407). We have carefully addressed all the points raised, and our point-to-point responses are detailed below. Reviewer comments are shown in blue. Our responses are shown in black. The revised texts are shown in red.

Major Comments

1. Limited Optimization Period:

The top-down optimization was performed only for four months (each season). Please justify why the analysis was limited to these periods and discuss whether this may affect annual emission estimates or bias seasonal interpretations.

Response:

Thank you for your valuable comment. Our primary reason for adopting the representative-month approach was to enable a robust independent validation of our results, which is a common practice in computationally intensive modeling studies (Qu et al., 2017; Xia et al., 2025; Xu et al., 2021). By constraining our emissions using only four months, the remaining eight months serve as an independent dataset against which we can evaluate the performance of our posterior inventory. The good performance of our posterior simulation (including 'non-training' months) provides strong evidence that the adjustments are not over-fitted to specific monthly conditions and that the resulting posterior emission inventory is effective for the entire season.

Second, the use of representative months is a reasonable approach for characterizing seasonal patterns. The representative months effectively capture the overall seasonal cycle, with the highest concentrations in summer and the lowest in winter. Furthermore, the NH_3 column concentration of each representative month is in good agreement with its corresponding three-month seasonal average, with the relative difference ranging from only 1.9% to 17.3%. This small discrepancy confirms that our method reliably represents the seasonal average.

Furthermore, conducting year-round simulations for emission adjustments would incur substantial computational costs, which is a critical practical constraint. Our study

conducted more than 20 regression iterations to optimize emissions. Extending this process to 12 months would demand additional computational resources of ~14 model-years, representing an extremely resource-intensive undertaking for regional chemical modeling.

We have revised the methodology section to provide this comprehensive explanation.

Revision in Section 4.1:

The posterior emission inventory derived for each representative month was then applied to all three months within its corresponding season to generate the full 12-month posterior inventory. This representative-month approach was adopted to allow for a robust validation against the full 12-month period, with the remaining eight months serving as an independent dataset, and to manage the substantial computational cost of the iterative process.

2. **Validation with Surface Data:**

While Figure S2 attempts to demonstrate agreement between model and surface observations, a time series or seasonal comparison between observations at these sites and both prior and posterior simulations would provide more clarity. Consider including monthly or seasonal cycle plots at selected sites to demonstrate how well the posterior simulation captures temporal variability. Scatter plots comparing prior vs. observed and posterior vs. observed NH_3 concentrations (similar to Figures S4–S6) should be more clearly explained in the main text.

Response:

We thank the reviewer for this constructive feedback. In response to your suggestions, we have significantly expanded the validation section of our manuscript with more detailed seasonal comparisons.

The validation utilizes in situ surface NH_3 measurements from 13 sites within our study domain (detailed in Table S2), as reported by Pan et al. (2018) for the period from autumn 2015 to summer 2016. For a direct comparison, simulated surface concentrations were extracted from the corresponding model grids and aggregated to seasonal means.

Our analysis confirms a marked improvement with the posterior emissions. The annual mean surface NH_3 concentration from the posterior simulation (9.4 μg m^{-3}) is

substantially closer to the observed value (12.7 μg m^{-3}) than the prior (6.3 μg m^{-3}). As shown in Figure R3.1, this is quantified by a 42% reduction in the model's underestimation (MFB reduced by 0.42) and a higher Index of Agreement (IOA), indicating better spatial consistency.

As requested, we have enhanced the seasonal analysis, with detailed results now presented in Table R3.1. The prior simulation underestimated observed surface NH_3 by 37%–79% across seasons. The posterior simulation, while still showing some underestimation, significantly alleviates this bias and demonstrates better performance metrics (lower RMSE and higher IOA), thereby better capturing the seasonal characteristics.

We have also expanded the discussion on potential sources for the remaining discrepancy. This gap may be attributed to several factors: (1) our optimization was constrained by satellite total column densities, which may not perfectly translate to surface-level improvements; (2) a partial temporal mismatch exists between our 2016 simulation and the 2015–2016 observation period; and (3) extreme local conditions at certain sites, such as the exceptionally high summer concentrations at the Yucheng site, are inherently challenging for a regional model to capture.

Table R3.1 Seasonal comparison of simulated and observed surface NH_3 concentrations (μg m^{-3}) and associated statistical metrics.

	MAM	JJA	SON	DJF
Prior surface NH_3 concentration (μg m^{-3})	5.05	7.58	6.68	6.06
Observed surface NH_3 concentration (μg m^{-3})	11.48	17.53	12.48	9.26
IOA	0.49	0.54	0.66	0.67
MFB	-0.79	-0.74	-0.54	-0.37
RMSE (μg m^{-3})	8.29	13.06	7.64	5.76
	MAM	JJA	SON	DJF

Posterior surface concentration (μg m^{-3})	NH_3	8.86	10.10	9.13	9.44
Observed surface concentration (μg m^{-3})	NH_3	11.48	17.53	12.48	9.26
IOA		0.56	0.61	0.7	0.72
MFB		-0.24	-0.47	-0.19	0.12
RMSE (μg m^{-3})		5.86	10.63	6.13	5.08

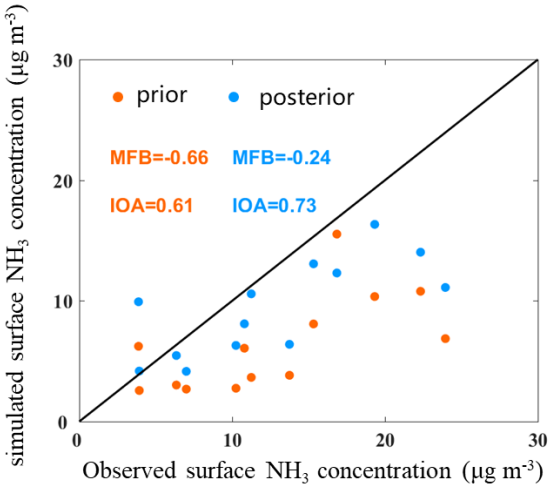

Figure R3.1 Scatter plot comparison of prior (orange) and posterior (blue) simulated seasonal mean surface NH_3 concentrations against in situ observations. The solid black line indicates the 1:1 ratio.

Revision in Section 4.3:

A similar improvement is also witnessed in the modeling of surface NH_3 concentrations, which were evaluated against in-situ measurements from 13 sites reported by Pan et al. (2018a) for the 2015–2016 period (Table S2). The posterior simulation significantly improves the annual mean, increasing the surface concentration from 6.3 μg m^{-3} (prior) to 9.4 μg m^{-3} (posterior), much closer to the observed average of 12.7 μg m^{-3}. As shown in the scatter plot in Figure S7, the posterior simulation alleviates the underestimation at most sites, which is quantified by a 42% reduction in the overall underestimation bias and a clear improvement in the IOA. On

a seasonal basis, the posterior emissions also alleviate the large underestimation of the prior simulation across all seasons, though the degree of improvement varies (Table S6). The prior simulation showed significant underestimation in all seasons, with the MFB ranging from -0.37 in winter to -0.79 in spring. The posterior simulation demonstrates a particularly evident improvement in spring, where the MFB reduced from -0.79 to -0.24. While some underestimation remains in summer, the posterior results still show improved performance metrics (e.g., lower RMSE and higher IOA) for all seasons, confirming a better capture of the seasonal characteristics overall. The remaining discrepancy between the posterior simulation and surface observations can be attributed to several factors, such as the spatial representativeness of the surface sites and the accuracy of the secondary inorganic aerosol simulation.

Revision in Supplementary:

Table S6 Seasonal comparison of simulated and observed surface NH_3 concentrations ($\mu g\ m^{-3}$) and associated statistical metrics.

	MAM	JJA	SON	DJF
Prior surface NH_3 concentration ($\mu g\ m^{-3}$)	5.05	7.58	6.68	6.06
Observed surface NH_3 concentration ($\mu g\ m^{-3}$)	11.48	17.53	12.48	9.26
IOA	0.49	0.54	0.66	0.67
MFB	-0.79	-0.74	-0.54	-0.37
RMSE ($\mu g\ m^{-3}$)	8.29	13.06	7.64	5.76
	MAM	JJA	SON	DJF
Posterior surface NH_3 concentration ($\mu g\ m^{-3}$)	8.86	10.10	9.13	9.44
Observed surface NH_3 concentration ($\mu g\ m^{-3}$)	11.48	17.53	12.48	9.26
IOA	0.56	0.61	0.7	0.72

MFB	*-0.24*	*-0.47*	*-0.19*	*0.12*
RMSE (μg m^{-3})	*5.86*	*10.63*	*6.13*	*5.08*

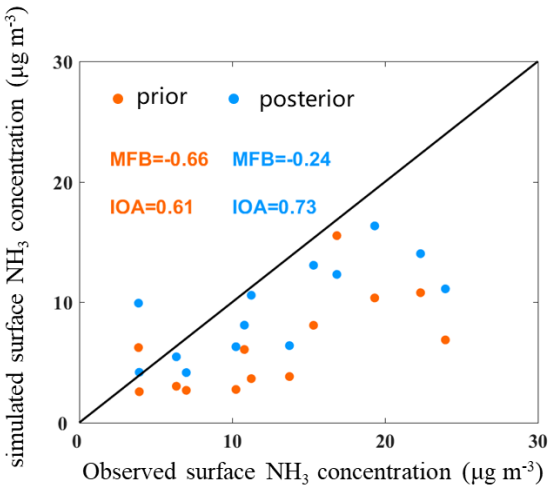

Figure S7 Scatter plot comparison of prior (orange) and posterior (blue) simulated seasonal mean surface NH_3 concentrations against in situ observations. The solid black line indicates the 1:1 ratio.

3. **Clarification on Posterior Emission Totals:**

Page 13, L343: Clarify whether the 4.2 Tg emission is derived from the posterior estimate. Given the remaining model–observation gap, this number should be framed as a lower-bound estimate. Please discuss the implications.

Response:

Thank you for this insightful suggestion. We have revised the manuscript to provide the requested clarification and context.

We confirm that the 4.2 Tg value represents the total annual NH_3 emission derived from our posterior estimate. Following your suggestion, we agree that this value should be framed as a conservative, lower-bound estimate due to the remaining gap between our model results and observations.

Our analysis shows that while the posterior emissions significantly improve the simulation, the resulting annual mean NH_3 total column density (23.7×10^{15} molec cm^{-2}) still lower than the satellite-retrieved value (29.0×10^{15} molec cm^{-2}). The implication of this discrepancy is that the true NH_3 emissions in this region may be even higher than our estimate. Fully closing this model-observation gap would likely require further

upward adjustments to the emission inventory. We have added a discussion to the manuscript to reflect this important context.

Revision in Section 6:

The posterior results indicate that the NH_3 emission in Eastern China for 2016 amounted to 4.2 Tg.

Revision in Section 4.2:

In similar years and regions, the discrepancy between the estimates of this study and other studies ranges from 1.0% to 19.6%. The slight discrepancy can be partially explained by our estimate being a conservative lower bound, a consequence of the residual gap remaining with satellite retrieval.

4. **Sectoral Emission Trends and Inconsistencies:**

Page 8, L216–218 and L223: There seems to be a discrepancy between the statements about non-AGR and AGR emission changes. Figure 5b suggests a spring increase, typically associated with agricultural activity, yet the larger change is attributed to non-AGR sources. Please clarify the partitioning of the emission increase.

Response:

We thank the reviewer for this important question. The partitioning of emission changes during spring is indeed complex, and we have expanded the discussion in the manuscript to provide a clearer explanation.

The significant increase in total spring emissions is the net result of adjustments in both agricultural (AGR) and non-agricultural (non-AGR) sectors. Our posterior analysis reveals substantial but spatially heterogeneous changes within the agricultural sector. For example, while AGR emissions in the Henan region were reduced to correct a prior overestimation, emissions in the Yangtze River Delta (YRD) concurrently increased by 242.8 Gg. Despite these regional adjustments, agriculture remains the dominant source in spring, accounting for 84.1% of total posterior emissions.

However, to bridge the large gap between prior simulations and satellite observations, a significant upward adjustment in total emissions was necessary. While annual AGR emissions were adjusted upwards, non-agricultural sources required an even more greater revision, driven by the spatial patterns of NH_3 concentrations. Given the high NH_3 level observed during spring, a large portion of the seasonal emission increase was attributed to the non-AGR sector to better match the observations.

Key non-AGR sources contributing to this increase include industrial processes (e.g., "ammonia slip" from emission controls), vehicle emissions (a byproduct of three-way catalysts), and waste management (volatilization from landfills and wastewater treatment). Rising spring temperatures can enhance the volatilization rates from several of these sources, leading to considerable emissions. We have incorporated this detailed explanation into the revised manuscript.

Revision in Section 4.2:

The seasonal variations in the posterior emissions is the net result of complex adjustments in both the AGR and non-AGR sectors.

5. **Loss of High Emission Feature in SON/DJF (Figure 6):**

The high-emission feature at the intersection of Henan, Hebei, and Shandong disappears in SON and DJF seasons. Please explain whether this is due to real seasonal changes or limitations in the model/data.

Response:

Thank you for your careful observation. We have revised the manuscript to address this important point.

First, we would like to clarify that the high-concentration feature at the intersection of Henan, Hebei, and Shandong does persist through autumn and winter in both the satellite retrievals and our posterior simulation. The concentration in this region remains significantly higher than in surrounding areas during these seasons. To better visualize this, we have revised Figure 6 with an adjusted color scale, which now clearly shows the high-value center in the posterior simulation, consistent with the satellite observations.

However, we acknowledge that a gap between our posterior simulation and the satellite data still exists in the colder seasons. This residual bias is likely due to methodological limitations. One potential factor is our iterative stopping criterion, which concludes the optimization when the mean error is reduced to 30%. This inherent tolerance allows for a certain level of discrepancy to remain. Another factor is that our optimization was performed monthly, which may introduce inconsistencies when results are aggregated and evaluated on a seasonal scale.

Despite these limitations, the posterior result represents a significant improvement over the prior simulation. We have added an expanded discussion on these

methodological uncertainties to the text to provide a more transparent and robust analysis.

Revision in Section 4.3:

In summary, the posterior simulation improves the agreement between the simulated NH_3 column concentrations and satellite observations in both overall magnitude and spatial distribution, although some deviations remain, particularly in the colder seasons. These can likely be attributed to methodological limitations, such as the inherent tolerance of our 30% iterative stopping criterion and potential inconsistencies from aggregating monthly optimizations to a seasonal scale.

6. **Surface Bias Reduction (Page 10, L277–278):**

Clarify which observational data were used (in situ surface measurements vs. satellite), whether the bias reduction is spatially averaged, and if supporting plots are available. A comparison showing seasonal variation would strengthen this claim.

Response:

Thank you for this constructive suggestion. We have revised the manuscript to provide the requested clarifications.

The validation was performed using in situ surface NH_3 measurements from a network of 13 sites within our study domain, as reported by Pan et al.(2018). This dataset provides seasonal mean concentrations from autumn 2015 to summer 2016. Site details are available in Table S2.

The reduction in bias is observed on both a spatially averaged and a site-by-site basis. The supporting analysis is presented in Figure R3.1, which includes scatter plots comparing both prior and posterior simulations against the observations. These plots clearly demonstrate that the posterior simulation alleviates the underestimation at most sites.

Following your suggestion, we have also strengthened the seasonal comparison. The revised manuscript and its supplement (Table S6) now explicitly compare simulated and observed seasonal NH_3 concentrations. The results confirm that our posterior inventory leads to a more consistent performance and reduced bias across all four seasons, as quantified by improved MFB and IOA metrics.

Revision in Section 4.3:

A similar improvement is also witnessed in the modeling of surface NH_3

concentrations, which were evaluated against in-situ measurements from 13 sites reported by Pan et al. (2018a) for the 2015–2016 period (Table S2). The posterior simulation significantly improves the annual mean, increasing the surface concentration from 6.3 μg m^{-3} (prior) to 9.4 μg m^{-3} (posterior), much closer to the observed average of 12.7 μg m^{-3}. As shown in the scatter plot in Figure S7, the posterior simulation alleviates the underestimation at most sites, which is quantified by a 42% reduction in the overall underestimation bias and a clear improvement in the IOA. On a seasonal basis, the posterior emissions also alleviate the large underestimation of the prior simulation across all seasons, though the degree of improvement varies (Table S6). The prior simulation showed significant underestimation in all seasons, with the MFB ranging from -0.37 in winter to -0.79 in spring. The posterior simulation demonstrates a particularly evident improvement in spring, where the MFB reduced from -0.79 to -0.24. While some underestimation remains in summer, the posterior results still show improved performance metrics (e.g., lower RMSE and higher IOA) for all seasons, confirming a better capture of the seasonal characteristics overall. The remaining discrepancy between the posterior simulation and surface observations can be attributed to several factors, such as the spatial representativeness of the surface sites and the accuracy of the secondary inorganic aerosol simulation.

7. Table 3 Description (Page 11, L288–297):

Provide more detail on the meaning of the single values listed in Table 3. What metrics are these? How do they compare across seasons and sectors?

Response:

We thank the reviewer for this helpful suggestion. We have revised the manuscript to provide a more detailed description of Table 3.

The values in Table 3 represent the annual mean concentrations of $PM_{2.5}$, SO_2, and NO_2 derived from the prior simulation, the posterior simulation, and surface observations. The observational data were averaged from 80 monitoring sites across 9 major cities (details in Table S4). The comparison was performed by matching the observed data from each site with the simulated concentration from its corresponding

model grid cell.

Regarding the comparison, both simulations capture the pollutant concentrations reasonably well, with the posterior results showing a clear improvement. This is particularly evident for SO_2, where the posterior simulated concentration is much closer to the observed value, reducing the model's previous overestimation by 27%. This improvement is most significant in autumn, as the increased availability of NH_3 in our posterior simulation drives more gaseous SO_2 into the particle phase. This more detailed description has been added to the main text.

Revision in Section 4.3:

Furthermore, improving the NH_3 simulation results in the other simulated air pollutants being closer to observed levels (Table 3). Specifically, we compare the annual mean concentrations of $PM_{2.5}$, SO_2, and NO_2 from the prior and posterior simulations against surface observations averaged from 80 monitoring sites across 9 major cities (Table S4).

A similar improvement is also observed for SO_2, where the posterior simulated concentration (6.8 ppbv) better matches the observed value (6.5 ppbv), reducing the model's previous overestimation by 27%. This improvement is most significant in autumn. The successful capture of air pollutants highlights a significant improvement in the NH_3 emission inventory for Eastern China.

8. **Public Health and $PM_{2.5}$ Impact:**

Page 11, L306: Quantify the reduction in $PM_{2.5}$ (1.5–5.7 μg/m³) as a percentage of baseline concentrations to help contextualize the health impact.

Response:

Thank you for this detailed suggestion. We agree that providing percentages helps to contextualize the impact of NH_3 emission reductions. We have revised the relevant section of the manuscript to incorporate these values.

Revision in Section 5:

Figure 7 illustrates that reducing NH_3 emissions by 30%–60% can decrease the seasonal $PM_{2.5}$ concentrations by 1.5–5.7 μg m^{-3} (2.0%–7.2%) averaged for Eastern China in winter, mainly due to the reduction in SIA.

Minor Comments

• **Page 4, L97:** Surface data usage should be mentioned in the abstract for completeness.

Response: Thank you for the suggestion. We have revised the abstract accordingly.

Revision in Abstract:

The optimized NH_3 emission significantly improved the simulation of both total column and surface NH_3 concentrations, with improvements in magnitude (31%–42%) and variations (17%–55%).

• **Page 7, L164:** Briefly explain the extreme values of IOA and MFB to aid reader interpretation.

Response: We appreciate this helpful comment and have expanded the text to briefly explain the interpretation of these metrics for the reader.

Revision in Section 3:

The IOA quantifies the overall model skill, where a value of 1 indicates a perfect match and 0 denotes complete disagreement. The MFB diagnoses systematic model bias, where positive values indicate overestimation, negative values indicate underestimation, and 0 signifies no average bias.

• **Page 7, L180–184:** Confirm whether these lines are referencing Figure 6.

Response: Thank you for pointing this out. We have revised the text to add the explicit reference to Figure 6.

Revision in Section 3:

As illustrated in Figure 6, satellite-based observations reveal that the spatial high-value areas of NH_3 column are located at the junction of Henan, Shandong, and Hebei provinces. In contrast, the prior modeling results show that NH_3 column densities are more concentrated in Henan. This indicates a clear discrepancy in the spatial distribution of NH_3 column densities between the prior simulations and the observations.

• **Page 8, L201:** Remove extra period after "Table 2."

Response: Thank you for pointing this out. The text has been corrected.

• **Page 9, L239:** Correct grammar: "based on both top-down and bottom-up approaches."

Response: Thank you for the suggestion. The text has been revised as recommended.

Revision in Section 4.2:

Overall, the estimated NH_3 emission in this study is comparable to the estimates of the other studies based on both "top-down" and "bottom-up" approaches.

• **Page 10, L265:** Suggest adding the prior result value alongside the percentage difference for clarity.

Response: Thank you for this helpful suggestion. We agree that adding the prior result value improves clarity and have revised the sentence accordingly.

Revision in Section 4.3:

The annual mean simulated NH_3 total column density improved from the prior result of 17.4×10^{15} molec cm^{-2} to a posterior value of 23.7×10^{15} molec cm^{-2}, with an increase of 35.9%, and is closer to the observed value of 29.0×10^{15} molec cm^{-2}.

• **Page 11, L281:** Reword the statement to reflect partial improvement in posterior vs. surface observations.

Response: Accepted. The relevant section of the manuscript has been updated to provide further clarification.

Revision in Section 4.3:

On a seasonal basis, the posterior emissions also alleviate the large underestimation of the prior simulation across all seasons, though the degree of improvement varies (Table S6). The prior simulation showed significant underestimation in all seasons, with the MFB ranging from -0.37 in winter to -0.79 in spring. The posterior simulation demonstrates a particularly evident improvement in spring, where the MFB reduced from -0.79 to -0.24. While some underestimation remains in summer, the posterior results still show improved performance metrics (e.g., lower RMSE and higher IOA) for all seasons, confirming a better capture of the seasonal characteristics overall.

• **Page 13, L342:** Add missing period.

Response: Thank you for noting this. The correction has been made.

Revision in Section 6:

In this study, we used IASI satellite products and an iterative algorithm with the WRF-Chem model to optimize the bottom-up NH_3 emission inventory for Eastern China

and further assessed the impacts of NH_3 emission reductions from different sources on $PM_{2.5}$ concentrations.

• **Page 13, L348:** Consider providing a geophysical or socioeconomic explanation (e.g., dense agriculture and livestock) for high emissions at the provincial intersection.

Response:

Thank you for this valuable suggestion. We have expanded the discussion in the manuscript to provide a geophysical and socioeconomic explanation for this high-emission hotspot, as requested.

The high NH_3 emissions at the intersection of these provinces are driven by two primary factors. First, this region is part of the North China Plain, characterized by intensive agriculture (both crop production and animal husbandry) and significant industrial activity, leading to exceptionally high emission intensity.

Second, topography plays a crucial role. The region is bordered by the Taihang and Yanshan Mountains, forming a semi-enclosed plain. This topography can obstruct the dispersal of air pollutants under certain meteorological conditions, leading to their accumulation in the piedmont area and the formation of a persistent high-concentration center.

Revision in Section 6:

Spatially, the region with the highest NH_3 emissions was located at the intersection of Henan, Hebei, and Shandong provinces. This is attributed to a combination of high emission intensity from dense agricultural and industrial activities and topographical effects that hinder the dispersal of pollutants.

Suggestions for Figures

• **Figure 2:** Add a row showing differences (posterior – prior) for better visualization of emission changes by sector.

Response: Thank you for this helpful suggestion. We have added a figure in the Supplementary to express the spatial difference in emissions by sector before and after optimization. Our iterative algorithm optimizes emissions on a regional basis to best match the satellite's observed spatial patterns, rather than applying a uniform scaling factor across the domain. This methodological approach results in heterogeneous adjustments, leading to the significant spatial differences observed between provinces, with increases in some areas and decreases in others to achieve an optimal overall fit.

Revision in Supplementary:

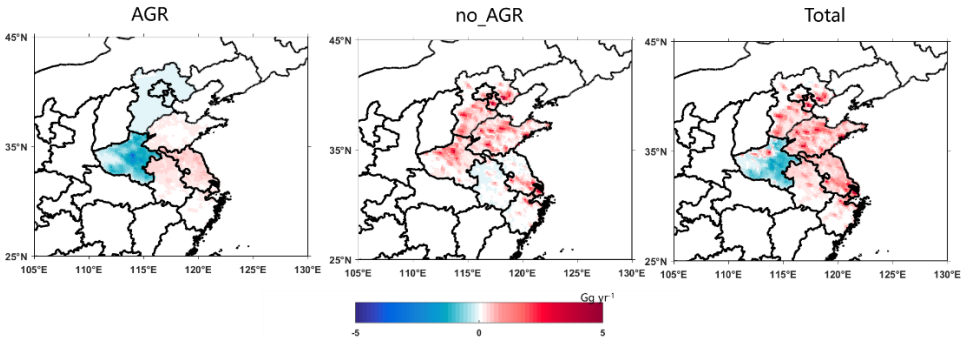

Figure S4. Spatial distribution of the difference in NH_3 emissions (Posterior − Prior) for AGR and non-AGR sources.

• **Figure 3:** Clarify what the red box highlights; also discuss large underestimates in Shandong and BTH.

Response:

Thank you for these suggestions. We have revised the manuscript to improve the clarity of Figure 3 and to expand the discussion.

First, we have clarified the meaning of the red box in the figure caption. The box highlights the range we consider to represent good model performance, specifically where the RMSE is less than 10 ($\times 10^{15}$ molec cm^{-2}) and the simulated-to-observed ratio is between 0.7 and 1.3 (i.e., within a ±30% margin).

Second, regarding the underestimation in certain regions, our analysis confirms that this residual bias is most pronounced during the autumn season. We have added a discussion attributing this remaining discrepancy to the inherent limitations of our

inversion methodology. Potential factors include our iterative stopping criterion (a 30% error tolerance) and inconsistencies arising from aggregating monthly optimizations to a seasonal scale. This discussion provides a more transparent assessment of our results.

Revision in Figure 3:

Figure 3. *Scatter plots of the prior and posterior NH_3 total column data versus IASI retrievals. Each point represents prior (or posterior) data for a specific season and a specific region. Circles, triangles, rhombuses, and rectangles correspond to the BTH, Henan, Shandong, and YRD regions, respectively. Orange and blue markers represent a prior and a posterior data, respectively. The red box indicates the performance area, with a model error within ±30% and an RMSE below 10($\times 10^{15}$ molec cm^{-2}).*

Revision in Section 4.3:

In summary, the posterior simulation improves the agreement between the simulated NH_3 column concentrations and satellite observations in both overall magnitude and spatial distribution, although some deviations remain, particularly in the colder seasons. These can likely be attributed to methodological limitations, such as the inherent tolerance of our 30% iterative stopping criterion and potential inconsistencies from aggregating monthly optimizations to a seasonal scale.

• **Figure 6:** Add units to the color bar for clarity.

Response: Thank you for the suggestion. The units have been added to the color bar in Figure 6.

• **Figure S2:** Increase font size on color bar units.

Response: Thank you for the comment. We have increased the font size on the color bar units in Figure S2 as requested.

References

• Please ensure that all relevant IASI-based ammonia studies are cited appropriately to position your work in the broader context of satellite-based NH_3 retrievals and applications.

Response: We appreciate this guidance. To better position our study within the broader context of the field, we have incorporated citations to several additional relevant IASI-

based NH_3 studies in the revised manuscript.

References

Pan, Y., Tian, S., Zhao, Y., Zhang, L., Zhu, X., Gao, J., Huang, W., Zhou, Y., Song, Y., Zhang, Q., and Wang, Y.: Identifying Ammonia Hotspots in China Using a National Observation Network, Environ Sci Technol, 52, 3926–3934, https://doi.org/10.1021/acs.est.7b05235, 2018.

Qu, Z., Henze, D. K., Capps, S. L., Wang, Y., Xu, X., Wang, J., and Keller, M.: Monthly top-down NO_x emissions for China (2005–2012): A hybrid inversion method and trend analysis, JGR Atmospheres, 122, 4600–4625, https://doi.org/10.1002/2016JD025852, 2017.

Xia, J., Zhou, Y., Fang, L., Qi, Y., Li, D., Liao, H., and Jin, J.: South Asia ammonia emission inversion through assimilating IASI observations, https://doi.org/10.5194/egusphere-2024-3938, 20 January 2025.

Xu, M., Jin, J., Wang, G., Segers, A., Deng, T., and Lin, H. X.: Machine learning based bias correction for numerical chemical transport models, Atmospheric Environment, 248, 118022, https://doi.org/10.1016/j.atmosenv.2020.118022, 2021.